THE JOURNAL OF PHYSICAL CHEMISTRY A

 VOLUME 104, NUMBER 5, FEBRUARY 10, 2000

LETTERS

The Role of Dark States in the Photodynamics of the Green Fluorescent Protein Examined with Two-Color Fluorescence Excitation Spectroscopy

G. Jung, S. Mais, A. Zumbusch,* and C. Bräuchle

Institut für Physikalische Chemie and Center for Nanoscience, Ludwig-Maximilians-Universität München, Butenandtstrasse 5-13 (Haus E), 81377 München, Germany

Received: August 19, 1999; In Final Form: October 27, 1999

The green fluorescent protein (GFP) and its mutants are important fluorescent markers for the microscopy of biological specimens. Their photodynamics are governed by transitions between the neutral and anionic form of the light emitting chromophore. We used two-color fluorescence excitation spectroscopy to show that this is also true for mutants such as EGFP and E222Q, which in their ground state do not show any absorption attributable to the neutral chromophore. The photodynamics of E222Q are described within the framework of a 4-level system comprising two dark states. Two-color fluorescence correlation spectroscopy (FCS) has been employed to determine the rate constants for this system. The first of these states has a population rate of 3×10^5 s^{-1} and a lifetime of 50 μs, indicating that this is the triplet state. The second state, which we identified as the neutral chromophore, has a population rate of 4×10^5 s^{-1} and a lifetime of 500 μs. Our data allude to the fact that, already at low intensities, a large fraction of the molecules are in the dark states.

1. Introduction

The green fluorescent protein (GFP) of the jellyfish *Aequorea victoria* consists of 238 amino acids.[1] Its chromophore is 4-(p-hydroxybenzylidene)imidazolidin-5-one (Figure 1), which is formed in an autocatalytic posttranslational cyclization of the residues Ser65Tyr66Gly67.[2] GFP has attracted a lot of attention as it is so far the only genetically encodeable fluorescent protein.[3] Wild-type GFP has a characteristic double absorption at 400 and 475 nm, respectively. X-ray structural investigations[4] and ultrafast spectroscopical studies[5,6] show that this is due to the chromophore existing in either a neutral form or as an anion. Meanwhile many mutants of GFP have been produced with different spectroscopical properties. These mutants have been classified by Tsien into seven different classes depending on the exact nature of their chromophores,[7] where the main difference is the relative stability of the neutral and the anionic form of the fluorophore in the protein. Bulk measurements[8] and single molecule experiments performed in our own laboratory show that GFP is subject to easy bleaching in comparison to fluorescent dyes commonly used as labels. This is unexpected as the X-ray structural analysis shows that the chromophore is protected from contact with reactive species by the surrounding protein matrix, which forms a β-can.[9,10] Single-molecule experiments may hold the key to understanding the observed bleaching behavior. The former reveal a strong blinking in the fluorescence of individual GFP molecules,[11−13] which leads to a decrease in the absolute fluorescence count rate. In experiments with YFP (a yellow fluorescent mutant with an anionic chromophore) Dickson et al. observed that fluorescence can be recovered after bleaching by using a short wavelength illumination at 405 nm,[12] which corresponds to the absorption band of the neutral form. Furthermore, the photochemical conversion of the chromophore from the neutral into its anionic form was observed in bulk experiments.[5] In summary, these observations indicate that

* To whom correspondence should be directed.

10.1021/jp992937w CCC: $19.00
Published on Web 01/19/2000

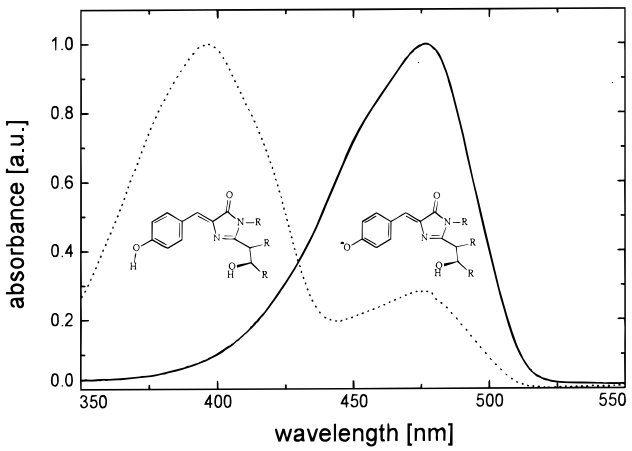

Figure 1. Absorption spectrum of GFP mutant E222Q (solid line, pH 10) and wt-GFP (dotted line, pH 7). The wt-GFP spectrum shows two maxima corresponding to the neutral chromophore (λ_{max} near 400 nm) and to the anionic chromophore (λ_{max} near 475 nm), whereas the mutant E222Q exhibits only one peak as expected for class II GFP mutants. The different states of the chromophore are shown in the insets.

photochemically driven transitions between the anionic and neutral forms of the chromophore are present in many GFP mutants.

In this letter we present the results obtained from two-color experiments with GFP in aqueous solution. By exciting the two absorption bands of GFP at 407 and 476 nm simultaneously, we can influence the fluorescence dynamics, increase the fluorescence yield, and determine the transition rates from one state to the other. To examine bulk samples we applied fluorescence excitation spectroscopy, while on the single-molecule level we used fluorescence correlation spectroscopy (FCS). FCS enables us to investigate dynamical processes of single molecules on a time scale between 100 ns to 1 ms.[14] FCS offers two advantages over other single molecule detection techniques. It allows proteins to be examined in solution under quasi native conditions, while meaningful data can already be obtained from short fluorescence traces. Recently results of FCS experiments on GFP at different pH values have been published.[15] Two-color FCS experiments with simultaneous fluorescence excitation of two different dyes have been reported by Eigen and co-workers.[16] New to our approach is the usage of a second laser excitation source as an external parameter to probe one chromophore.

2. Experimental Section

2.1. Setup and Materials. The experimental setup is based on a confocal microscope as used in single-molecule studies.[14] Light from a Kr^+ laser (407 nm) was overlapped with light from an Ar^+ laser (476 nm) and coupled into an inverted microscope (Nikon, TE-300). All excitation light was reflected off a dichroic mirror (Chroma, 485 DCXR) and focused with an NA 1.2 water-immersion lens (Nikon, Plan Apo 60x). The fluorescence light was collected with the same objective and the background light was reduced using a confocal pinhole (diameter 50 or 100 μm). Emission filters (Omega, 535DF55 or Chroma, HQ 510/50) were used to further suppress residual excitation light. For saturation experiments, the fluorescence light was detected with a single photon counting module (EG&G Canada, SPCM-AQR-14) and a photon counting system (Stanford Research, SR 400). For the FCS experiments, the fluorescence signal was divided by a 50:50 beam splitter and detected with two separate modules to avoid artifacts due to afterpulsing of the avalanche photodiodes.[14] The autocorrelation function was determined with a correlator (ALV Langen, ALV-5000/F). Fluorescence lifetime measurements were done using a F900 fluorescence spectrometer from Edinburgh Instruments.

EGFP (F64L/S65T) was obtained from Clontech (Palo Alto, CA), wt-GFP and mutant E222Q were kindly provided by J. Wiehler and B. Steipe (Genzentrum, LMU Munich). In the mutant E222Q, glutamic acid at position 222 is replaced by glutamine, which interrupts the H-bonding framework and stabilizes the anionic form of the chromophore. The fluorescence maximum of E222Q is at 506 nm and the fluorescence quantum yield is approximately 50%. The protein solutions ($>10^{-5}$ M) were further diluted with air-saturated water (Sigma, HPLC-grade) and with 20 mM buffer solution (Fluka, pH 10, HPCE-grade) to yield 5×10^{-9} M solutions appropriate for single-molecule detection in FCS experiments or 10^{-7} M solutions for bulk measurements.

3. Results and Discussion

3.1. Bulk Saturation Experiments. GFP mutants have more or less pronounced short and long wavelength absorptions corresponding to their chromophores being in the neutral or the anionic form. Figure 1 depicts the absorption spectra of wt-GFP and E222Q. A short wavelength absorption often leads to fluorescence that is red shifted by more than 100 nm relative to the excitation wavelength. This can be explained by a fast excited state proton transfer, so that the emitting species electronically resembles a molecule with an anionic chromophore.[17] Usually the molecules will be protonated again after emission of a photon. There is, however, a small probability that the chromophore in its neutral state may relax into the anionic state after excitation. Likewise the reverse process might be observed by exciting the chromophore in the anionic state.

Our aim was to examine whether class II GFP molecules such as E222Q, with a stabilized anionic chromophore, change their protonation state upon photoexcitation. Therefore we performed fluorescence excitation experiments by simultaneously exciting at 476 nm and at 407 nm, which enables us to address both states of the chromophore at the same time. The integrated fluorescence intensity was determined after blocking light with a wavelength < 507 nm. Using a second excitation source with a wavelength that is absorbed by the photoproduct of the 476 nm irradiation, an increase in fluorescence was observed, which was larger than the sum of the fluorescence count rates for both of the illumination sources applied separately. This can either be due to a reconversion of the photoproduct into its original state or due to the fluorescence of the photoproduct itself. Figure 2 shows the fluorescence intensity for the mutants E222Q and EGFP. The illumination intensity I^{476} at 476 nm was held constant, while the illumination intensity I^{407} at 407 nm was gradually increased. The subsequent increase in fluorescence is saturable at low intensities of 407 nm excitation. Assuming absorption coefficients and fluorescence yields for the state absorbing at 407 nm, which are typical for the GFP chromophore, it is obvious that the direct excitation of the fluorescence from this state affords only a negligible contribution to the observed increase in fluorescence.

The latter has therefore to be attributed to an efficient reconversion of the photoproduct. The observed saturation behavior can be described using the following model:[18]

$$R(I^{407}) = R_0^{476} + \mathrm{BG}(I^{407}) + \Delta R_\infty^{407} \times \frac{I^{407}}{I^{407} + I_S^{407}} \quad (1)$$

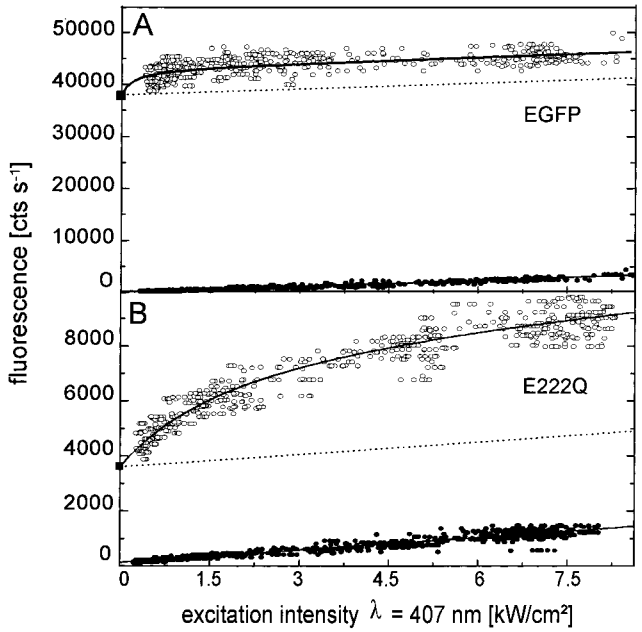

Figure 2. Total fluorescence count rate in the two-color saturation experiments with EGFP (**A**, 3×10^{-8} M, pH 10) and E222Q (**B**, 1×10^{-8} M, pH 10). Solid circles: single color excitation at 407 nm. Open circles: two color excitation at 407 nm with a fixed intensity of 7.6 kW cm^{-2} at 476 nm. Data for solely illuminating at 476 nm were taken in separate measurements (solid squares). The solid lines are curves fitted to the data as explained in the text. The dotted lines represent the offsets due to single-color excitation.

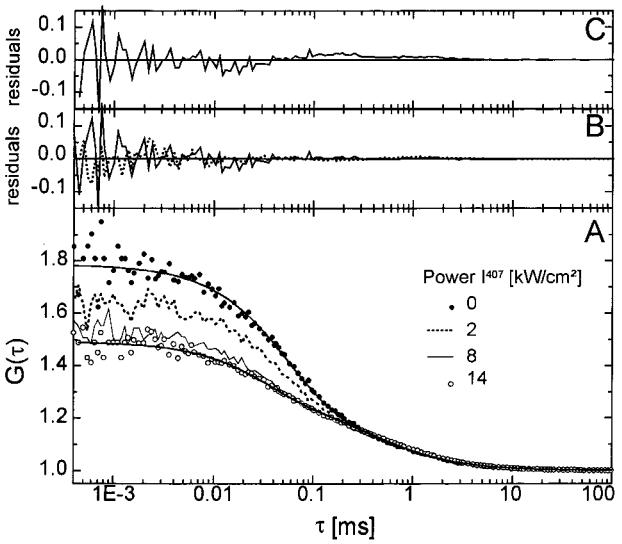

Figure 3. Two-color fluorescence autocorrelation functions of the mutant E222Q (pH 10, fixed intensity at 476 nm of 23 kW cm^{-2}). **A** shows the curves obtained for different excitation intensities at 407 nm. The solid lines represent fits calculated according to eq 2. The lower curve is obtained using a monoexponential fitting function for the intramolecular dynamics (residuals as a dotted line in **B**). Data for excitation solely at 476 nm are shown as the uppermost curve in **A**. Fits to this curve require a biexponential fitting function (residuals as a solid line in **B**). The large errors resulting in attempts to use a monoexponential fitting function can be seen as large residuals depicted in **C**.

where $R(I^{407})$ is the total detected fluorescence count rate and R_0^{476} is the offset fluorescence due to the irradiation at 476 nm. The count rate measured by solely illuminating at 407 nm is BG(I^{407}). We find that in experiments with class II GFP mutants such as EGFP and E222Q, the background BG(I^{407}) rises linearly with the excitation power at 407 nm, as expected for pure scattering. ΔR_∞^{407} denotes the maximum fluorescence count rate increase. The saturation intensity I_S^{407} is defined as the power necessary for obtaining half the maximum value of the increase.

The spectra of E222Q and EGFP indicate no significant absorption near 400 nm in the equilibrium at pH 10. However, for an additional illumination at 407 nm we observed a maximum increase in fluorescence yield of 140 (±10)% with a saturation intensity I_S^{407} of 2.5 kW/cm^2 for E222Q. For EGFP we detected only a slight increase of 13 (±3)% with a saturation intensity I_S^{407} that was below 1 kW/cm^2 (Figure 2). The observed increase in fluorescence yield when using an additional illumination source allowed us to estimate the relative proportion of the GFP molecules with their chromophores in the neutral or the anionic state. In the case of E222Q the increase of 140% corresponds to a 60% population of the photoproduct state for an intensity of 7.6 kW/cm^2 at 476 nm.

Wt-GFP is a class I mutant, in which the neutral and the anionic form of the chromophore are present in the ground state. At low excitation intensities it also showed an increase in fluorescence yield when subject to dual color illumination. However, a detailed analysis of this increase is impossible, as fluorescence can either originate from direct excitation or from excitation after prior conversion. For this reason wt-GFP was not investigated any further in the experiments described here.

3.2. Fluorescence Correlation Spectroscopy (FCS). The GFP mutant E222Q showed the largest effects in the bulk two-color saturation experiments, so we decided to focus the FCS measurements on this mutant. The underlying principles of FCS have been described in several excellent review articles.[19,20] In brief, FCS allows us to calculate the autocorrelation function from the fluorescence signal of a small number of molecules diffusing through a well defined excitation volume. At low enough concentrations of the sample solutions, fluctuations in the fluorescence intensity can be observed. These are caused either by a differing number of molecules in the laser focus or by intramolecular on/off dynamics of individual molecules such as transitions into the triplet state. FCS shares some of the properties of a single molecule detection technique, as the features in a correlation function vanish with an increase in the number of molecules. The analysis of the correlation function can supply information about the concentration of the solution, the diffusion coefficients and the molecular rate constants into and out of the dark states. To extract the characteristic parameters we compared the measured correlation functions (Figure 3A) with the following theoretical expression, which was similarly used in ref 15:

$$G(\tau) = \frac{\langle I(t) \times I(t+\tau)\rangle}{\langle I(t)\rangle^2} = 1 + \frac{1}{N}\left(1 + \frac{\tau}{\tau_D}\right)^{-1} \times (1 + C_1 \times e^{-\lambda_1 \tau} + C_2 \times e^{-\lambda_2 \tau}) \quad (2)$$

The first part of the product in eq 2 is the general expression accounting for translational diffusion within the 2-dimensional model.[21] This model is applicable for our setup, which encompasses tightly focused laser beams with Gaussian intensity profiles perpendicular to the optical axis and a large detection pinhole that results in a smooth field gradient along the optical axis. The contribution of diffusion along the optical axis is therefore negligible. N is the average number of fluorescence emitting molecules diffusing through the sample volume, and τ_D is related to the lateral beam waist ω in the focal plane and

the diffusion coefficient D by the equation $\tau_D = \omega^2/4D$. The factor ω, which was determined to be 340 nm, and D, which depends only on the viscosity of the solution and the shape and size of the chromophore, had to be the same for each measured correlation curve. D was found to be 8.2 ($\pm$0.5) 10^{-7} cm^2/s.

The last bracket in eq 2 represents the influence of the intramolecular dynamics. For the experiments without an excitation at 407 nm, fitting the experimental data with only one exponential function led to unacceptable deviations (Figure 3C). To obtain a more faithful representation of the measured values, a further exponential term is required in the fitting function, which leads to the general expression in eq 2. A sum of two exponential terms is characteristic for correlation functions of a four-level system.[22] Two of these levels are the ground and fluorescing excited states, the other two levels are dark states. The contrasts C_1 and C_2 and the rates λ_1 and λ_2 generally depend on all of the transition rates in the four-level system and can be calculated by solving the rate equations. However, the analytical solutions are complex and do not lend themselves to a fitting procedure.

Exploiting the photophysical behavior of GFP, which was observed in the bulk experiments, one can simplify the system by using a second excitation color. In agreement with the bulk saturation experiments we found that one of the observed dark states is sensitive to excitation at 407 nm. An increase in the excitation intensity at 407 nm results in a decreasing contrast of the correlation functions for the short time processes (see Figure 3).

Even at comparatively low intensities of 407 nm excitation, correlation functions were obtained which can be fitted with a monoexponential term for the bracket 2 in eq 2. This necessitates an effective depopulation of one of the dark states. Transitions into and out of this state are no longer observable, so that the related contrasts in the correlation functions vanish. The complexity of the system was now reduced to a three-level system. In this case (with $C_2 = 0$) the contrast C_1 and the rate λ_1 are defined by the effective rate into and out of the remaining dark state:[14,23]

$$C_1 = \frac{k_{23}^{\text{eff}}}{k_{31}} \tag{3}$$

$$\lambda_1 = k_{31} + k_{23}^{\text{eff}}$$

$$k_{23}^{\text{eff}} = k_{23}\frac{k_{12}}{k_{12} + k_{21}}$$

The rate constant k_{12} for absorption is proportional to the intensity of the 476 nm light, and k_{21} is the inverse fluorescence lifetime of the excited singlet state. For this calculation the fluorescence lifetime for E222Q was measured to be 2.5 ns, while absorption cross-sections for typical class II mutants were taken from Tsien.[7] The rates k_{23} and k_{31} can be determined by varying the excitation intensity at 476 nm. For low excitation intensities, λ_1 corresponds to the inverse lifetime of the dark state. The rate constant k_{23} was obtained from the slope of the function for the dependence of λ_1 on the excitation intensity at 476 nm (Figure 4). We determined k_{31} to be 2×10^4 s^{-1} ($\pm$10%) and k_{23} to be 3×10^5 s^{-1} ($\pm$40%). The lifetime of about 50 μs of this state is a value typical for triplet states.

Knowing the rates of the three-level system, we fitted the biexponential curves obtained without the 407 nm irradiation. In the limit of low intensity excitation at 476 nm, the rate constants are separate in eq 2. The rate constant k_{41} is now equal to λ_2 and was determined to be 2×10^3 s^{-1} ($\pm$50%). For moderate to high illumination intensities however a more precise treatment of the four-level system is necessary. This analysis will be published in a forthcoming article.[24] From the low intensity data we could estimate k_{24} to have a value in the order of 4×10^5 s^{-1}. The absorption properties indicate that this dark state may be a form of the neutral chromophore with an average lifetime of about 500 μs.

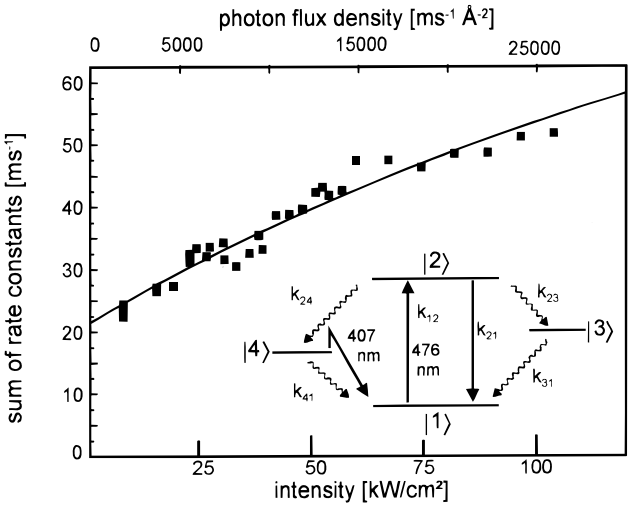

Figure 4. Dependence of the sum of the rate constants $k_{31} + k_{23}^{\text{eff}}$ on the intensity of 476 nm excitation (407 nm excitation in saturation). The inset shows the scheme for the four-level system. Conversion of state 4 into state 1 after 407 nm excitation takes place via an unidentified excited state. The exact nature of this state has no implication for the calculation of the rate constants presented here.

As a class II GFP mutant, E222Q has its chromophore stabilized in the anionic state with no detectable absorption of the neutral chromophore. The experimental data show that, despite this fact, the neutral chromophore plays an important role in the photodynamics of the protein. A similar effect, if not as dramatic, was observed for the widely used mutant EGFP. Our results imply that the values for the absorption coefficients and the quantum yields at least for class II GFP mutants are intensity dependent. Especially in microscopic experiments these proteins might yield less fluorescence than expected. Already at the moderate intensities of 8 kW/cm^2 at 476 nm, approximately 70% of the E222Q molecules will be in the dark states. Of these, 65% are in the neutral chromophore state and around 5% are in the triplet state. Higher intensities will further deplete the concentration of the fluorescing molecules. One way to circumvent this problem may be to use a second excitation color to efficiently depopulate the neutral state of the chromophore.

4. Conclusion

We presented two-color fluorescence excitation bulk measurements of different GFP mutants. The increase in observed fluorescence count rate, when simultaneously using a second excitation source, initiated a series of two-color fluorescence correlation experiments mainly of the E222Q mutant. In these experiments the second color was used as an external parameter to probe the population dynamics of the different states of one GFP molecule. We found that although E222Q is a class II mutant with no observable steady state absorption around 400 nm, the neutral state of the chromophore with an excitation maximum around 400 nm was efficiently populated when exciting at 476 nm. A second dark state of the molecule,

presumably its triplet state, was also observed. Performing intensity-dependent measurements we were able to determine the rate constants for transitions in the resulting four-level system. The results give an insight into the complex photophysics of GFP and indicate how to improve the fluorescence yield in experiments using GFP as a fluorescent label.

Acknowledgment. We thank J. Wiehler and B. Steipe for supplying us with the GFP mutants and A. Hards for proofreading the manuscript. Financial support by the Deutsche Forschungsgemeinschaft is gratefully acknowledged.

References and Notes

(1) Prasher, D. C.; Eckenrode, V. K.; Ward, W. W.; Prendergast, F. G.; Cormier, J. *Gene* **1992**, *111*, 229.
(2) Cody, C. W.; Prasher, D. C.; Westler, W. M.; Prendergast, F. G.; Ward, W. W. *Biochemistry* **1993**, *32*, 1212.
(3) Chalfie, M.; Tu, Y.; Euskirchen, G.; Ward, W. W.; Prasher, D. C. *Science* **1994**, *263*, 802.
(4) Brejc, K.; Sixma, T. K.; Kitts, P. A.; Kain, S. R.; Tsien, R. Y.; Ormö; M.; Remington, S. J. *Proc. Natl. Acad. Sci. U.S.A.* **1997**, *94*, 2306.
(5) Chattoraj, M.; King, B. A.; Bublitz, G. U.; Boxer, S. G. *Proc. Natl. Acad. Sci. U.S.A.* **1996**, *93*, 8362.
(6) Lossau, H.; Kummer, A.; Heinecke, R.; Pollinger-Dammer, F.; Kompa, C.; Bieser, G.; Jonsson, T.; Silva, C. M.; Yang, M. M.; Youvan, D. C.; Michel-Beyerle, M. E. *Chem. Phys.* **1996**, *213*, 1.
(7) Tsien, R. Y. *Annu. Rev. Biochem.* **1998**, *67*, 509.
(8) Patterson, G. H.; Knobel, S. M.; Sharif, W. D.; Kain, S. R.; Piston, D. W. *Biophys. J.* **1997**, *73*, 2782.
(9) Ormö, M.; Cubitt, A. B.; Kallio, K.; Gross, L. A.; Tsien, R. Y.; Remington, S. J. *Science* **1996**, *273*, 1392.
(10) Yang, F.; Moss, L. G.; Phillips, G. N., Jr. *Nature Biotech.* **1996**, *14*, 1246.
(11) Pierce, D. W.; Horn-Booher, N.; Vale, R. D. *Nature* **1997**, *388*, 338.
(12) Dickson, R. M.; Cubitt, A. B.; Tsien, R. Y.; Moerner, W. E. *Nature* **1997**, *388*, 355.
(13) Jung, G.; Wiehler, J.; Göhde, W.; Tittel, J.; Basché, T.; Steipe, B.; Bräuchle, C. *Bioimaging* **1998**, *6*, 54.
(14) Widengren, J.; Mets, Ü.; Rigler, R. *J. Phys. Chem.* **1995**, *99*, 13368.
(15) Haupts, U.; Maiti, S.; Schwille, P.; Webb, W. W. *Proc. Natl. Acad. Sci. U.S.A.* **1998**, *95*, 13573.
(16) Kettling, U.; Koltermann, A.; Schwille, P.; Eigen, M. *Proc. Natl. Acad. Sci. U.S.A.* **1998**, *95*, 1416.
(17) Bublitz, G.; King, B. A.; Boxer, S. G. *J. Am. Chem. Soc.* **1998**, *120*, 9370.
(18) Ambrose, W. P.; Basché, T.; Moerner, W. E. *J. Chem. Phys.* **1991**, *95*, 7150.
(19) Eigen, M.; Riegler, R. *Proc. Natl. Acad. Sci. U.S.A.* **1994**, *91*, 5740.
(20) Maiti, S.; Haupts, U.; Webb, W. W. *Proc. Natl. Acad. Sci. U.S.A.* **1997**, *94*, 11753.
(21) Rigler, R.; Mets, Ü.; Widengren, J.; Kask, P. *Eur. Biophys. J.* **1993**, *22*, 169.
(22) Boiron, A. M.; Lounis, B.; Orrit, M. *J. Chem. Phys.* **1996**, *105*, 3969.
(23) Bernard, J.; Fleury, L.; Talon, H.; Orrit, M. *J. Chem. Phys.* **1993**, *98*, 850.
(24) Jung, G.; Mais, S.; Zumbusch, A.; Bräuchle, C., in preparation.